Penetration of Amphiphilic Quantum Dots through Model and Cellular Plasma Membranes

6 AUTHORS, INCLUDING:

Aliaksei Dubavik
ITMO University
16 PUBLICATIONS **247** CITATIONS

SEE PROFILE

Erdinc Sezgin
University of Oxford
28 PUBLICATIONS **331** CITATIONS

SEE PROFILE

Petra Schwille
Max Planck Institute of Biochemistry
334 PUBLICATIONS **15,829** CITATIONS

SEE PROFILE

Alexander Eychmüller
Technische Universität Dresden
**356** PUBLICATIONS **10,800** CITATIONS

SEE PROFILE

Penetration of Amphiphilic Quantum Dots through Model and Cellular Plasma Membranes

Aliaksei Dubavik,[†,‡,||] Erdinc Sezgin,[§,⊥,||] Vladimir Lesnyak,[†,*] Nikolai Gaponik,[†] Petra Schwille,[§] and Alexander Eychmüller[†]

[†]Physical Chemistry, TU Dresden, Bergstrasse 66b, 01062 Dresden, Germany, [‡]Photonics and Optoelectronics Group, Department of Physics and CeNS, Ludwig-Maximilians-Universität München, Amalienstrasse 54, 80799 Munich, Germany, [§]Biophysics Group, BIOTEC, TU Dresden, Tatzberg 47-51, 01307 Dresden, Germany, and [⊥]Max Planck Institute for Molecular Cell Biology and Genetics, Pfotenhauerstrasse 108, 01307 Dresden, Germany. [||]These authors contributed equally to this work.

Owing to their unique photophysical properties, colloidal semiconductor nanocrystals or quantum dots (QDs) are promising tools for biolabeling, bioimaging, and bioanalysis instead of, or in combination with, fluorescent organic dyes and biomolecules.[1−6] In comparison to organic fluorophores, QDs exhibit many advantages, such as broad absorption and narrow emission spectra, a wide spectral range, long lifetimes, high molar extinction coefficients, and photostability and chemical stability.[7] Nevertheless, some issues still need to be addressed for their successful application as biomarkers, one of which is the intracellular delivery of colloidal nanoparticles. While organic dyes used for tracking intracellular events are able to permeate cell membranes, the size and surface properties of QDs prevent their diffusion across the lipid bilayer.[8] QDs often end up in endocytic compartments instead of their individual delivery into cell organelles. Therefore, strategies to eliminate the endocytic pathway, described, for example, for negatively charged thioglycolic acid (TGA)-capped CdTe QDs,[9] and to diffuse through the cell membrane as individual units should be developed. From this point of view, nanoparticles showing good solubility in water, high colloidal stability, quite small sizes, and at the same time a low surface charge which prevents the particles from aggregation *via* interaction with various countercharged species always present in biological media, should be appropriate candidates for biolabeling experiments. In addition, an ideal candidate is expected to exhibit also compatibility with media of different polarity, for instance, hydrophilic (water) and hydrophobic (lipids) ones.

ABSTRACT
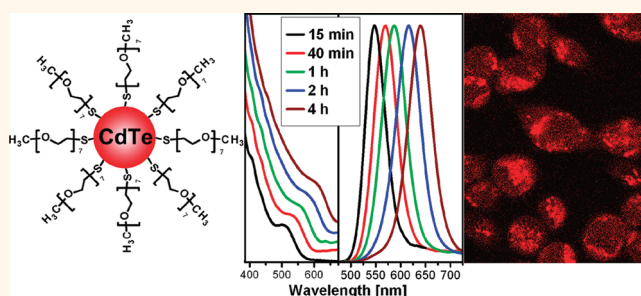
In this work we demonstrate progress in the colloidal synthesis of amphiphilic CdTe nanocrystals stabilized by thiolated PEG oligomers with the aim of facilitating cellular uptake of the particles. High-boiling, good coordinating solvents such as dimethylacetamide and dimethylformamide accelerate the growth of the nanoparticles yielding stable colloids of which photoluminescence maxima can be tuned to cover the region of 540−640 nm with quantum yields of up to 30%. The CdTe nanocrystals capped by thiolated methoxypolyethylene glycol are shown to penetrate through the lipid bilayer of giant unilamellar vesicles and giant plasma membrane vesicles which constitute basic endocytosis-free model membrane systems. Moreover, the penetration of amphiphilic particles through live cell plasma membranes and their ability to escape the endocytic pathway have been demonstrated.

KEYWORDS: amphiphilic CdTe nanocrystals · colloidal synthesis · photoluminescence · giant unilamellar vesicles · giant plasma membrane vesicles · penetration through the cell membrane · endocytosis

One of the most useful model systems to study membrane related processes in a controlled fashion is the giant unilamellar vesicle (GUV). GUVs are spherical membranes generated by an electroformation using natural or synthetic lipids and they are used in several applications mimicking the cell membrane.[10] However, as they have limited compositional elements, a more advanced membrane system, the giant plasma membrane sphere (GPMV), has been developed. GPMVs are vesicles derived from a native cell membrane by

paraforlmaldehyde and dithiothreitol treatment.[11] Very recently both GUVs and GPMVs have been revealed as valuable model membrane systems to study the membrane penetration process.[12−14]

In this work, we report on further improvements of the synthesis of amphiphilic CdTe QDs which was introduced in ref 15. Using low-molecular-weight methoxypolyethylene glycol terminated with a HS-group (mPEG-SH) as the stabilizer leads to an inherent amphiphilicity of the nanoparticles.[15,16] Employing solvents of high polarity and high boiling temperatures in the synthesis yields nanocrystals exhibiting emission maxima ranging from 540 to 640 nm and photoluminescence quantum yields (PL QY) of up to 30%. These particles satisfy the basic requirements for bioimaging agents as mentioned above. Therefore, for the first time we show that these amphiphilic QDs are able to permeate through the endocytosis-free membrane systems, GUVs, and GPMVs. Moreover, experiments on live cells reveal the capability of the amphiphilic particles to diffuse through the cell membrane escaping the endocytic uptake that makes them perspective candidates for tracking whole cells and intracellular processes.

RESULTS AND DISCUSSION

As shown in our recent work, the synthesis of amphiphilic CdTe QDs capped by thiolated methoxypolyethylene glycol (CdTe@mPEG-SH) performed in toluene or water could deliver only relatively small nanocrystals of up to ∼2 nm in size with an emission maximum of ∼550 nm. This small size suggests that the conditions of the synthesis permit only an initial growth of the particles *via* a coalescence mechanism when small clusters and nuclei agglomerate to form larger particles while strongly retarding their further growth. Using the same synthetic strategy in this work but, instead of water and toluene, employing solvents with higher boiling temperatures, dimethylformamide (DMF) and dimethylacetamide (DMA) (t_{bp} of DMF = 153.1 °C, t_{bp} of DMA = 166.1 °C)[17] yields CdTe QDs with average diameters of up to ∼4 nm emitting in the wide visible spectral region from 540 to 640 nm with a QY of up to 30%. The absorbance and PL spectra of CdTe@mPEG-SH colloids grown in DMA are shown in Figure 1. Interestingly, in DMA the growth of the nanoparticles is 9 times faster than that in DMF (the PL maxima of 640 nm were reached in 4 h for the reaction in DMA and in 36 h for DMF) while the difference between the boiling temperatures of these solvents is only 13 °C (see above). This observation suggests that besides the temperature of the reaction mixture, the solvation capability of the medium toward the precursors and the evolving nuclei plays an important role as well. DMA and DMF are known as coordinating solvents which act as electron-donors and thereby are good
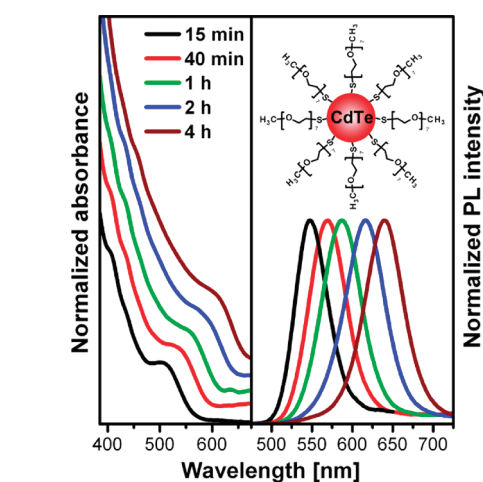

Figure 1. Absorbance and PL ($\lambda_{ex.}$ = 450 nm) spectra of CdTe@mPEG-SH QDs synthesized in DMA as a function of the reflux time. Absorption spectra are shifted for clarity. The inset is a sketch of a CdTe particle capped by mPEG-SH.

cation solvators.[17] Thus, DMA having the higher boiling point, a larger donor number, and dielectric constant in comparison with DMF (27.8 and 26.6 kcal·mol^{-1}, 37.78 and 36.71, respectively[17]), facilitates the growth of the CdTe nanocrystals. Such a large growth rate leads to a relatively broad size distribution of the CdTe@mPEG-SH QDs in comparison with that from an aqueous synthesis; however the PL full width at half-maximum of the amphiphilic particles is quite comparable to those obtained in water and lies in the range of 48−59 nm. The transmission electron microscopy (TEM) image of the nanocrystals shown in Figure SI1 (see the Supporting Information) demonstrates their broad size distribution and reveals their good crystallinity. Applying size-selective precipitation (as described in detail in ref 18) using a toluene/hexane (1/3) mixture as the nonsolvent allows for the separation of several QD fractions with narrower size distributions. The presence of differently sized particles is proven also by PL excitation (PLE) spectra (see Supporting Information, Figure SI2). In contrast to absorption and PL measurements, PLE enables the user to distinguish between several species within an ensemble. The quite irregular (nonspherical) shapes and the broad size distribution of the nanoparticles observed by TEM suggest that most probably coalescence is the main growth mechanism of the particles in DMF (or DMA) which are built-up from a number of small species like nuclei and/or clusters. The low zeta potential (see below) facilitates the agglomeration of the small species owing to their reduced electrostatic repulsion. The evolution of the absorption maxima of the QDs during the reaction time (see Supporting Information, Figure SI3) which is indicative for their size evolution does not show any clear transition from the coalescence mechanism into Ostwald ripening which has been shown, for example, for aqueous TGA-capped CdTe nanocrystals.[19] It is

noted that although the irregular shapes and the relatively broad size distribution may be considered as disadvantageous the obtained nanoparticles offer two desired functionalities necessary for the membrane penetration experiments described below, namely a widely tunable emission and the amphiphilicity. Indeed, as demonstrated in our previous work[15] for green emitting amphiphilic nanoparticles larger orange emitting CdTe@mPEG-SH QDs synthesized both in DMA and in DMF exhibit a similar spontaneous 3-phase transfer from toluene *via* water to chloroform confirming their unique amphiphilic properties (see Supporting Information, Figure SI 4).

The synthetic approach described above leading to larger amphiphilic QDs with tunable PL with maxima reaching 640 nm greatly extends the opportunities for applications in bioimaging experiments since this allows for a proper choice of a QD-dye pair for an efficient separation of their PL signals. For membrane penetration experiments orange QDs emitting with a maximum at 610 nm and red QDs emitting with a maximum at 634 nm were chosen in order to distinguish their luminescence from the green emitting membrane dye 3,3′-dioctadecyloxacarbocyanine perchlorate (DiO). As a control sample, hydrophilic CdTe crystals stabilized with TGA having a similar size (*ca.* 3 nm) were used in parallel permeation experiments. The optical characteristics of the orange emitting samples are shown in Figure 2. CdTe@TGA QDs carry deprotonated carboxyl groups on their surface and hence possess negative charge. Zeta potential measurements reveal a value of −65 mV. On the contrary, amphiphilic CdTe nanoparticles have a slightly positive zeta potential of 4 mV which favors their versatile solubility and should prevent aggregation *via* electrostatic interaction in biological media (see below). As opposed to ligand exchange procedures, the stable bonding of the stabilizer to the nanocrystal surface imparts a high colloidal stability against deterioration. The short chain length of the $H_3C(OCH_2CH_2)_7SH$ molecule assures the quite small sizes of the resulting nanoparticles which is also beneficial for biological applications.

To test the ability of the QDs to permeate through lipid bilayers, GUVs prepared in sucrose *via* electroformation were incubated in phosphate buffered saline (PBS) containing amphiphilic and hydrophilic (as a control sample in parallel tests) particles in equal concentrations. Confocal microscopy images obtained during 3 h are shown in Figure 3 where the red background stems from the QD fluorescence and the black circles are interiors of the "empty" GUVs. The uptake was quantified during a period of 3 h by acquiring the intensity profile of the inner part of the GUVs. The intensities of the QD fluorescence background and the empty GUVs have also been quantified as references (see Figure 3). More than 100 GUVs have been
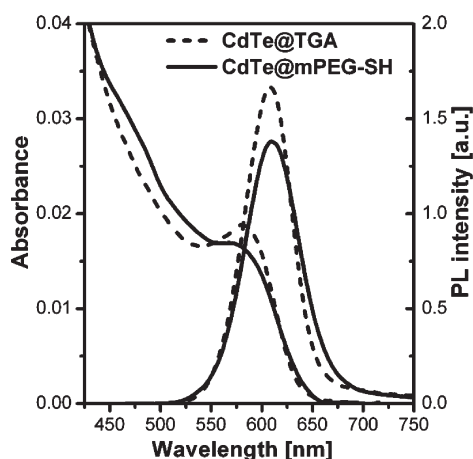

Figure 2. Absorbance and PL ($\lambda_{ex.}$ = 450 nm) spectra of the amphiphilic CdTe@mPEG-SH QDs and the hydrophilic CdTe@TGA QDs colloids used for the GUV experiment.
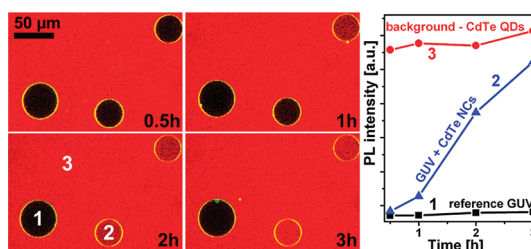

Figure 3. Confocal microscopy images acquired after 0.5, 1, 2, and 3 h of incubation of GUVs with CdTe@mPEG-SH QDs in PBS (left); corresponding emission intensity profiles of the regions of interest shown on the left (right). The black cycles (*e.g.*, no. 1) are "empty" vesicles which do not contain QDs, while the red ones (*e.g.*, no. 2) contain penetrated QDs. The intensity and the contrast were adjusted for better visualization.

observed in order to estimate the uptake efficiency after 3 h and overnight incubation. Approximately 40% of the GUVs contained QDs after 3 h, while after overnight incubation this number increased to 60%. Many parameters such as membrane curvature, size of the vesicle, unilamellarity of the membrane, and lipid packing may account for the heterogeneous penetration. It should be noted that even after overnight exposure the QDs still have retained their emission. In the control experiment performed with CdTe@TGA QD colloids no penetration was observed presumably because of their aggregation (see Figure SI 4) which was also reported previously for TGA-capped CdTe QDs in PBS.[20] We also note that only lowering of the pH of the CdTe QDs colloid down to approximately 7 (from the initial 9−10) already leads to a slow destabilization and subsequent aggregation of the particles.

We further tested the colloidal stability of both types of QDs in various buffers (*cf.* also Boldt *et al.*[21]) including PBS, GPMV buffer, MEM cell medium, and air buffer which are the main buffers used for cellular maintenance (see Supporting Information, Table SI1). The experiments revealed that the amphiphilic
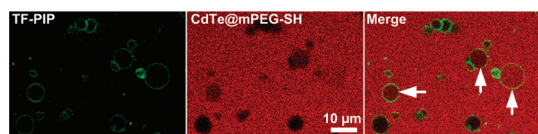
Figure 4. Confocal microscopy images, acquired after 3 h of incubation, demonstrating the penetration of the CdTe@m-PEG-SH QDs into GPMVs visualized by merging (right panel) the TF-PIP dye green fluorescence (left panel) and the QD red emission (middle panel). The arrows show the vesicles containing QDs. The black GPMVs are "empty" vesicles which do not contain QDs while the red ones contain penetrated QDs. The intensity and the contrast were adjusted for better visualization.

CdTe@mPEG-SH crystals remain homogenously dispersed in all the biological buffers while the hydrophilic CdTe@TGA QDs tend to aggregate in all of them (see Supporting Information, Figure SI5) presumably due to the interaction with Ca and Mg ions present in all the media. A controlled clustering of negatively charged CdTe@TGA particles by interconnection *via* Ca^{2+} ions acting as electrostatic chelating linkers was previously demonstrated by Mayilo *et al.*[22] It is considered that aggregation/clustering on the cell surface results in endocytosis[23] which is most probably the main reason why the hydrophilic nanoparticles cannot escape the endocytic uptake. However, our data show that in contrast to hydrophilic particles, the amphiphilic QDs do not form aggregates in the buffers mentioned and, thus, have the ability to diffuse through the GUV membrane preserving their colloidal stability in biological media.

To further investigate the penetration of the amphiphilic QDs we used GPMVs composed of a natural cell membrane as an intermediate model membrane system between the entirely artificial GUVs and a real live cell plasma membrane. Clear visualization of the QD permeation was achieved employing a two channel detection approach where the vesicle membrane has been visualized with the green emission of the Top-Fluor-phosphatidylinositol phosphate (TF-PIP), a membrane lipid dye incorporated into the membrane (see Figure 4) whereas the QD distribution in the system has been monitored *via* the red band-pass filters. As seen from the resulting merged image (Figure 4), the vesicles take up the amphiphilic nanocrystals during incubation. Although the penetration was slower than in the case of the GUVs we observed approximately 40% of GPMVs containing QDs after 10 h of incubation.

After proving the penetration of the amphiphilic CdTe@mPEG-SH QDs into the endocytosis-free synthetic model membrane system (GUVs) and a cell-derived membrane system (GPMVs) we have tested their permeation also in living cells. After 1 h of incubation of the cells with both CdTe@mPEG-SH and CdTe@TGA particles the penetration has been observed by confocal microscopy. Endosomes containing fluorescing molecules were shown to appear

as bright fluorescent spots inside the cells.[24] As seen from Figure 5, several bright spots which are the endosomes containing QDs were formed inside the cells incubated with hydrophilic CdTe@TGA particles, whereas only a few dim spots were observed inside the cells incubated with amphiphilic CdTe@mPEG-SH QDs. Moreover, there was almost no fluorescence signal inside the cells except that from the endosomes in cells exposed to the CdTe@TGA nanocrystals, while intense fluorescence from free nonclustered particles was observed in cells exposed to the CdTe@mPEG-SH nanocrystals which presumably originates from the QDs having penetrated individually through the membrane. The intensity of the endosome signal also shows that CdTe@TGA QDs were exclusively endocytosed, which makes the vesicles emit brighter while the CdTe@mPEG-SH containing vesicles are relatively dimmer due to the small fraction of the nanocrystals confined inside the endosomes. Although the occurrence of both direct penetration and endocytosis has been proposed for several molecules such as cell penetrating peptides[25] and retroviral particles,[26] the complete physicochemical mechanism is not yet thoroughly elucidated.

In an additional experiment, Alexa-488-labeled Transferrin which is taken up by clathrin/dynamin dependent endocytosis[27,28] was used to visualize the localization of endocytotic vesicles and QDs. The high colocalization of the nanoparticles and Transferrin inside the cell shown in Supporting Information, Figure SI 6(a–d) proves that the QDs which cannot penetrate through the membrane individually are endocytosed. Moreover, we quantified the fluorescence intensity stemming from the free QDs inside the cells along a z-stack series of the cell to see whether the localization of the free particles inside the cell is homogeneous. Supporting Information, Figure SI 6e shows that the intensity remains relatively constant along the cell axis indicating a homogeneous distribution of the QDs within the cellular cytoplasm.

CONCLUSIONS

In this study, we have further improved the synthesis of amphiphilic CdTe@mPEG-SH nanocrystals *via* the use of the high-boiling coordinating solvents dimethylacetamide and dimethylformamide. The optimized procedure yields QDs in the size range from 2 to 4 nm, emitting in the wide visible region of 540–640 nm with enhanced quantum yield of up to 30%. The permeability test performed using GUVs and GPMVs for the first time demonstrated the ability of amphiphilic nanoparticles to penetrate through lipid bilayers. Further experiments performed on live cells demonstrate the nonendocytic uptake of the amphiphilic particles, while hydrophilic CdTe@TGA QDs were solely accumulated in endosomes. This makes
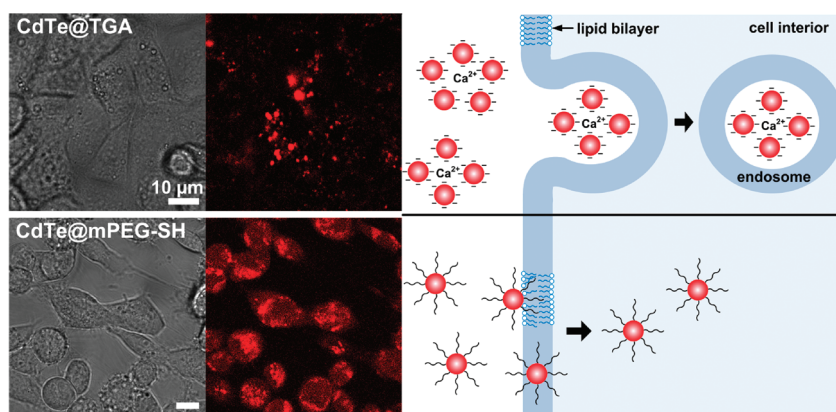
Figure 5. Bright field (left panels) and confocal microscopy (middle panels) images of live cells acquired after 1 h of incubation in the presence of CdTe@TGA (top) and CdTe@mPEG-SH (bottom) QDs demonstrating the distribution of the amphiphilic particles over the whole cell interiors with partial confinement in the endosomes and accumulation of the hydrophilic particles solely inside the endosomes. The intensity and the contrast were adjusted for better visualization. Simplified scheme of the penetration of the corresponding QDs into a cell (right panel). Lipids constituting the cell membrane are shown as a circle representing a hydrophilic head with a tail depicting their hydrophobic part.

CdTe@mPEG-SH QDs promising agents for tracking whole cells and intracellular processes. Moreover, their high colloidal stability in various biological media and stable emission properties can be exploited for a better delivery of agents for therapeutic applications. The data acquired also provide new insight into the interaction of nanoparticles with an artificial lipid membrane as well as with natural cell membranes.

EXPERIMENTAL SECTION

Synthesis of CdTe@mPEG-SH Nanocrystals. All chemicals used were of analytical grade or higher.

The short chain stabilizer $H_3C-(O-CH_2-CH_2)_7-SH$ was synthesized according to the method reported in refs 15 and 29.

The preparation of amphiphilic QDs was carried out both in DMA and in DMF solutions. In a typical synthesis, 0.16 g (0.69 mmol) of $Cd(CH_3COO)_2$ and 0.33 g (0.9 mmol) of mPEG-SH was dissolved in 30 mL of DMA (or DMF) followed by deaeration by argon bubbling for 30 min. Under vigorous stirring, H_2Te gas generated by the reaction of 0.1 g (0.228 mmol) of Al_2Te_3 lumps with an excess of 0.5 M H_2SO_4 solution was injected into the reaction mixture with a slow Ar flow. The molar ratio of Cd^{2+}/Te^{2-}/mPEG-SH was 1/1/1.3. Formation and growth of the nanoparticles proceeded upon reflux. The reaction was terminated after the PL maximum reached 640 nm (4 h in DMA, 36 h in DMF). Purification of the QDs was achieved by precipitation of the as-prepared colloidal solution of the CdTe nanoparticles from DMA or DMF by the addition of a toluene/hexane mixture (colloid/toluene/hexane = 1/1/3) followed by dissolution of the precipitate in pure solvent (e.g., water or toluene).

As a reference sample for the membrane permeability experiment, hydrophilic CdTe nanoparticles stabilized by TGA were prepared according to the procedure reported in ref 30. Prior to the GUV permeation experiment the CdTe@TGA nanoparticles were purified by a reprecipitation procedure as described in ref 18. Here we notice that various aspects of the aqueous synthesis of CdTe nanocrystals have been reviewed in recent publications.[31,32]

Characterization of CdTe@mPEG-SH Nanocrystals. UV–vis absorption spectra were collected with a Cary 50 spectrophotometer (Varian). Fluorescence spectra were measured using a FluoroMax-4 spectrofluorimeter (HORIBA Jobin Yvon). All spectra were taken at room temperature. The PL QYs of the QD solutions were determined according to the procedure described in ref 33 by comparison with Rhodamine 6G and Rhodamine 101 dyes in ethanol assuming their PL QYs to be 95% and 96%, respectively. Samples for TEM were prepared by dropping diluted nanoparticle solutions in toluene onto copper grids coated with a thin Formvar-carbon film with subsequent evaporation of the solvent. TEM images were obtained on a Tecnai T20 microscope (FEI), operating at 200 kV. The zeta-potentials were measured on a Beckman Coulter Delsa Nano C particle analyzer. The values were averaged from three measurements.

GUV Preparation. The GUV preparation by electroformation is described in detail in ref 34. Briefly, dioleoyl phosphatidylcholine (1,2-dioleoyl-sn-glycero-3-phosphocholine) (DOPC) (Avanti, AL, USA) and the membrane dye DiO (Invitrogen, CA, USA) were mixed in chloroform. Then this mixture was deposited on platinum wires. After chloroform evaporation, the platinum wires were dipped into sucrose solution and exposed to 10 Hz AC for 1 h and following 2 Hz AC for 30 min with a 2 V voltage.

For microscopy, the GUVs were mixed with PBS in Bovine Serum Albumin (BSA) coated LabTek chambers. Afterward, amphiphilic CdTe@mPEG-SH QDs and in parallel, as a control sample, hydrophilic CdTe@TGA QDs colloids (final concentration of 0.25 μM) were added to the chambers. The mixtures were incubated at room temperature.

GPMV Preparation. Chinese Hamster Ovary (CHO) cells were cultured in alpha MEM medium (for a description of the medium as well as for the buffers used see Supporting Information, Table SI1) supplemented with 10% Fetal Calf Serum up to 70–80% of confluence. GPMVs were isolated by chemically inducing cell blebbing with 25 mM paraforlmaldehyde and 2 mM dithiothreitol in GPMV buffer (150 mM NaCl, 10 mM Hepes and 2 mM $CaCl_2$ (pH 7.4)) for 1 h at 37 °C as previously described.[8] The membrane dye TopFluor PIP (Avanti, AL, USA) was added to GPMVs in a concentration of 0.1 μM. They were observed in BSA-coated Labtek chambers similar to GUVs. The mixtures were incubated at 4 °C.

Colloidal Stability Test. Equal concentrations of amphiphilic and hydrophilic QDs were mixed with the biological buffers listed in Table SI1 (see the Supporting Information), and subsequently imaged by confocal microscopy.

Cell Penetration Test. CHO cells were seeded on MatTek chambers (#1.5) and incubated in cell culture MEM medium supplemented with 10% Fetal Calf Serum up to 70–80% of confluence for 2 days at 37 °C. Afterward, equal amounts of amphiphilic and hydrophilic QDs (as a control sample in a parallel test) were added to the cell media (the final concentration was approximately 1 μM). The cells were incubated in QDs

containing media at 37 °C for an additional 1 h. Then, they were washed with PBS and observed with confocal microscopy in PBS. For the Transferrin endocytosis test, Alexa488-labeled Transferrin (Invitrogen, CA, USA) was added to the media with a final concentration of 5 μg/mL. The cells were washed after 5−10 min incubation at 37 °C.

Confocal Microscopy Imaging. Confocal microscopy images were acquired using a Zeiss LSM 510 microscope equipped with a 40X NA 1.2 UV−vis−IR C-Apocromat water-immersion objective and a 488 nm argon-ion laser. NFT 545 and NFT 635 filters were used to separate the green signals from the membrane dyes and from orange or red fluorescing QDs, respectively. For additional filtering, a band-pass 505−530 for green, a long pass 585 for orange, and a band-pass 615−685 for red emissions were employed. Imaging was performed in 0.5, 1, 2, and 3 h after QDs injection and after overnight incubation.

Conflict of Interest: The authors declare no competing financial interest.

Supporting Information Available: TEM image and PL excitation spectra of CdTe@mPEG-SH QDs; the evolution of the absorption maxima of the CdTe@mPEG-SH QDs during their growth; photographs demonstrating the spontaneous triphase transfer of CdTe@mPEG-SH nanocrystals; confocal microscopy images demonstrating the colloidal stability of the amphiphilic QDs in various cellular buffers and medium, as well as the colocalization of CdTe@mPEG-SH QDs and Alexa488-Transferrin in the cell cytoplasm, a table summarizing the cellular buffers and medium compositions and their main applications. This material is available free of charge *via* the Internet at http://pubs.acs.org.

REFERENCES AND NOTES

1. Michalet, X.; Pinaud, F. F.; Bentolila, L. A.; Tsay, J. M.; Doose, S.; Li, J. J.; Sundaresan, G.; Wu, A. M.; Gambhir, S. S.; Weiss, S. Quantum Dots for Live Cells, *in Vivo* Imaging, and Diagnostics. *Science* **2005**, *307*, 538–544.

2. Medintz, I. L.; Uyeda, H. T.; Goldman, E. R.; Mattoussi, H. Quantum Dot Bioconjugates for Imaging, Labelling and Sensing. *Nat. Mater.* **2005**, *4*, 435–446.

3. Rakovich, A.; Sukhanova, A.; Bouchonville, N.; Lukashev, E.; Oleinikov, V.; Artemyev, M.; Lesnyak, V.; Gaponik, N.; Molinari, M.; Troyon, M.; *et al*. Resonance Energy Transfer Improves the Biological Function of Bacteriorhodopsin within a Hybrid Material Built from Purple Membranes and Semiconductor Quantum Dots. *Nano Lett.* **2010**, *10*, 2640–2648.

4. Gill, R.; Zayats, M.; Willner, I. Semiconductor Quantum Dots for Bioanalysis. *Angew. Chem., Int. Ed.* **2008**, *47*, 7602–7625.

5. Liu, W.; Howarth, M.; Greytak, A. B.; Zheng, Y.; Nocera, D. G.; Ting, A. Y.; Bawendi, M. G. Compact Biocompatible Quantum Dots Functionalized for Cellular Imaging. *J. Am. Chem. Soc.* **2008**, *130*, 1274–1284.

6. Fu, A.; Gu, W.; Boussert, B.; Koski, K.; Gerion, D.; Manna, L.; Le Gros, M.; Larabell, C. A.; Alivisatos, A. P. Semiconductor Quantum Rods as Single Molecule Fluorescent Biological Labels. *Nano Lett.* **2007**, *7*, 179–182.

7. Resch-Genger, U.; Grabolle, M.; Cavaliere-Jaricot, S.; Nitschke, R.; Nann, T. Quantum Dots *versus* Organic Dyes as Fluorescent Labels. *Nat. Methods* **2008**, *5*, 763–775.

8. Derfus, A. M.; Chan, W. C. W.; Bhatia, S. N. Intracellular Delivery of Quantum Dots for Live Cell Labeling and Organelle Tracking. *Adv. Mater.* **2004**, *16*, 961–966.

9. Nabiev, I.; Mitchell, S.; Davies, A.; Williams, Y.; Kelleher, D.; Moore, R.; Gun'ko, Y. K.; Byrne, S.; Rakovich, Y. P.; Donegan, J. F.; *et al*. Nonfunctionalized Nanocrystals Can Exploit a Cell's Active Transport Machinery Delivering Them to Specific Nuclear and Cytoplasmic Compartments. *Nano Lett.* **2007**, *7*, 3452–3461.

10. Angelova, M. I.; Dimitrov, D. S. Liposome Electroformation. *Faraday Discuss. Chem. Soc.* **1986**, *81*, 303–311.

11. Scott, R. Plasma Membrane Vesiculation: A New Technique for Isolation of Plasma Membranes. *Science* **1976**, *194*, 743–745.

12. García-Sáez, A. J.; Ries, J.; Orzáez, M.; Pérez-Payà, E.; Schwille, P. Membrane Promotes tBID Interaction with BCL$_{XL}$. *Nat. Struct. Mol. Biol.* **2009**, *16*, 1178–1185.

13. Gordon, S. P.; Berezhna, S.; Scherfeld, D.; Kahya, N.; Schwille, P. Characterization of Interaction between Cationic Lipid−Oligonucleotide Complexes and Cellular Membrane Lipids Using Confocal Imaging and Fluorescence Correlation Spectroscopy. *Biophys. J.* **2005**, *88*, 305–316.

14. Säälik, P.; Niinep, A.; Pae, J.; Hansen, M.; Lubenets, D.; Langel, U.; Pooga, M. Penetration without Cells: Membrane Translocation of Cell-Penetrating Peptides in the Model Giant Plasma Membrane Vesicles. *J. Controlled Release* **2011**, *153*, 117–125.

15. Dubavik, A.; Lesnyak, V.; Thiessen, W.; Gaponik, N.; Wolff, T.; Eychmüller, A. Synthesis of Amphiphilic CdTe Nanocrystals. *J. Phys. Chem. C* **2009**, *113*, 4748–4750.

16. Dubavik, A.; Lesnyak, V.; Gaponik, N.; Eychmüller, A. One-Phase Synthesis of Gold Nanoparticles with Varied Solubility. *Langmuir* **2011**, *27*, 10224–10227.

17. Reichardt, C. *Solvents and Solvent Effects in Organic Chemistry*; Wiley-VCH Verlag GmbH & Co. KGaA: Weinheim, Germany, 2003; p 2063−2066.

18. Gaponik, N.; Talapin, D. V.; Rogach, A. L.; Hoppe, K.; Shevchenko, E. V.; Kornowski, A.; Eychmüller, A.; Weller, H. Thiol-Capping of CdTe Nanocrystals: An Alternative to Organometallic Synthetic Routes. *J. Phys. Chem. B* **2002**, *106*, 7177–7185.

19. Yin, S.; Huang, F.; Zhang, J.; Zheng, J.; Lin, Z. The Effects of Particle Concentration and Surface Charge on the Oriented Attachment Growth Kinetics of CdTe Nanocrystals in H$_2$O. *J. Phys. Chem. C* **2011**, *115*, 10357–10364.

20. Volkov, Y.; Mitchell, S.; Gaponik, N.; Rakovich, Y. P.; Donegan, J. F.; Kelleher, D.; Rogach, A. L. In-situ Observation of Nanowire Growth from Luminescent CdTe Nanocrystals in a Phosphate Buffer Solution. *ChemPhysChem* **2004**, *5*, 1600–1602.

21. Boldt, K.; Bruns, O. T.; Gaponik, N.; Eychmüller, A. Comparative Examination of the Stability of Semiconductor Quantum Dots in Various Biochemical Buffers. *J. Phys. Chem. B* **2006**, *110*, 1959–1963.

22. Mayilo, S.; Hilhorst, J.; Susha, A. S.; Höhl, C.; Franzl, T.; Klar, T. A.; Rogach, A. L.; Feldmann, J. Energy Transfer in Solution-Based Clusters of CdTe Nanocrystals Electrostatically Bound by Calcium Ions. *J. Phys. Chem. C* **2008**, *112*, 14589–14594.

23. Liu, A. P.; Aguet, F.; Danuser, G.; Schmid, S. L. Local Clustering of Transferrin Receptors Promotes Clathrin-Coated Pit Initiation. *J. Cell Biol.* **2010**, *191*, 1381–1393.

24. Macia, E.; Ehrlich, M.; Massol, R.; Boucrot, E.; Brunner, C.; Kirchhausen, T. Dynasore, a Cell-Permeable Inhibitor of Dynamin. *Dev. Cell* **2006**, *10*, 839–850.

25. Mano, M.; Teodósio, C.; Paiva, A.; Simões, S.; Pedroso de Lima, M. C. On the Mechanisms of the Internalization of S413-PV Cell-Penetrating Peptide. *Biochem. J.* **2005**, *390*, 603–612.

26. Isa, P.; Gutiérrez, M.; Arias, C. F.; López, S. Rotavirus Cell Entry. *Future Virol.* **2008**, *3*, 135–146.

27. Ehrlich, M.; Boll, W.; van Oijen, A.; Hariharan, R.; Chandran, K.; Nibert, M. L.; Kirchhausen, T. Endocytosis by Random Initiation and Stabilization of Clathrin-Coated Pits. *Cell* **2004**, *118*, 591–605.

28. Hanover, J. A.; Willingham, M. C.; Pastan, I. Kinetics of Transit of Transferrin and Epidermal Growth Factor through Clathrin-Coated Membranes. *Cell* **1984**, *39*, 283–293.

29. Shimmin, R. G.; Schoch, A. B.; Braun, P. V. Polymer Size and Concentration Effects on the Size of Gold Nanoparticles

Capped by Polymeric Thiols. *Langmuir* **2004**, *20*, 5613–5620.

30. Rogach, A. L.; Franzl, T.; Klar, T. A.; Feldmann, J.; Gaponik, N.; Lesnyak, V.; Shavel, A.; Eychmüller, A.; Rakovich, Y. P.; Donegan, J. F. Aqueous Synthesis of Thiol-Capped CdTe Nanocrystals: State-of-the-Art. *J. Phys. Chem. C* **2007**, *111*, 14628–14637.

31. Li, Y.; Jing, L.; Qiao, R.; Gao, M. Aqueous Synthesis of CdTe Nanocrystals: Progresses and Perspectives. *Chem. Commun.* **2011**, *47*, 9293–9311.

32. Gaponik, N.; Rogach, A. L. Thiol-Capped CdTe Nanocrystals: Progress and Perspectives of the Related Research Fields. *Phys. Chem. Chem. Phys.* **2010**, *12*, 8685–8693.

33. Grabolle, M.; Spieles, M.; Lesnyak, V.; Gaponik, N.; Eychmüller, A.; Resch-Genger, U. Determination of the Fluorescence Quantum Yield of Quantum Dots: Suitable Procedures and Achievable Uncertainties. *Anal. Chem.* **2009**, *81*, 6285–6294.

34. García-Sáez, A. J.; Carrer, D. C.; Schwille, P. Fluorescence Correlation Spectroscopy for the Study of Membrane Dynamics and Organization in Giant Unilamellar Vesicles. *Methods Mol. Biol.* **2010**, *606*, 493–508.